Benchmarking of De-noising Techniques for Streaking Artifacts in Industrial 3DXCT Scan Data

Hammad Qureshi,
SEECS, NUST,
H-12, Islamabad,
Pakistan.
hammad.qureshi@seecs.edu.pk

Muddassir Malik,
SEECS, NUST,
H-12, Islamabad,
Pakistan.
muddassir.malik@seecs.edu.pk

Malik Anas Ahmad
SEECS, NUST,
H-12, Islamabad,
Pakistan.
anas.ahmad@seecs.edu.pk

Christoph Heinzl
University of Applied Sciences
Upper Austria
Stelzhamerstraße 23
4600 Wels/Austria
Christoph.Heinzl@fh-wels.at

ABSTRACT

De-noising is one of the most important applications of image processing which has been applied to a wide variety of real world problems. De-noising allows for improving image quality in imaging modalities that are noise prone. A lot of research work has gone in to improving quality of 2D images using various de-noising techniques but new modalities of imaging such as industrial 3D X-ray computed tomography (3DXCT) have received little attention. Industrial 3DXCT scanning is used these days to acquire detailed images of the internal construction of industrial components and machinery so that defects within these can be identified non-destructively and non-intrusively. However, 3DXCT imaging is prone to artifacts and noise. One solution to the problem is to use increased number of projections which results in reduced noise but increased costs. A more cost effective solution is to de-noise the images. In this paper, we show how various de-noising techniques may be used to de-noise 3DXCT scan images acquired using a lower number of projections. We also benchmark these techniques using various picture quality measures. Our investigation shows that good results may be obtained using wavelet shrinkage and anisotropic diffusion.

Keywords

3D X-ray Computed tomography, 3D image de-noising, image enhancement.

1. INTRODUCTION

Industrial 3DXCT scanning is an emerging imaging technique that has revolutionized industrial inspection and quality control. 3DXCT scans are used to generate a highly accurate 3D image of industrial components and machinery, revealing important information about the internal material decomposition, density of the scanned material and internal construction of the scanned object. 3DXCT allows for non-destructive testing of industrial components for discovery of internal defects that are not possible to detect otherwise. Stress testing is usually used to detect such defects which often involves applying force on the object of interest which may lead to impairment of the machinery or industrial component. Using 3DXCT no stresses need to be applied on the object of interest and hence the technique can also be used to analyze elastic or deformable specimens. Moreover, industrial 3DXCT generates a 3D model that can be used to perform nominal comparisons between surface model of the scanned part and the corresponding CAD model, for assembly defect analysis, void analysis and can also be used for generation of CAD data for reverse engineering applications.

3DXCT scan inherently uses X-rays to acquire images of an object. The specimen is rotated and X-ray attenuation images are recorded typically at each angular step of a full rotation. This leads to a collection of X-ray images stored as a image stack. This image stack is subsequently used to reconstruct a 3D volumetric representation corresponding to the specimen being scanned. Although 3DXCT scanning has improved considerably since its invention, the technique still suffers from noise. The quality of the 3DXCT scan is directly dependent on the noise inherent in 3DXCT images, which has a strong

relation to the strength of the radiation used to acquire the images referred to as dose. Keeping the radiation low is of importance in the medical domain but in industrial 3DXCT high radiation poses no problems. However, there is a clear trend visible in industrial 3DXCT towards higher resolutions and smaller voxel sizes. Unfortunately due to this trend 3DXCT images tend to show increased levels of noise. A potential solution to the problem is the increased number of projections which results in reduction of noise but increases the cost of the scans greatly. Industrial 3DXCT images suffer from various types of noise, which includes streaking artifacts and beam hardening. Streaking artifacts are introduced due to limited detector dynamics as well as insufficient projection data or local highly changing attenuation coefficients of the scanned materials. Beam hardening is the result of the lower energy X-ray photons getting absorbed by the specimen being scanned. In this paper, we will only focus on removal of streaking artifacts. Figure 1 shows an example of streaking artifacts seen in a 3DXCT scan image.

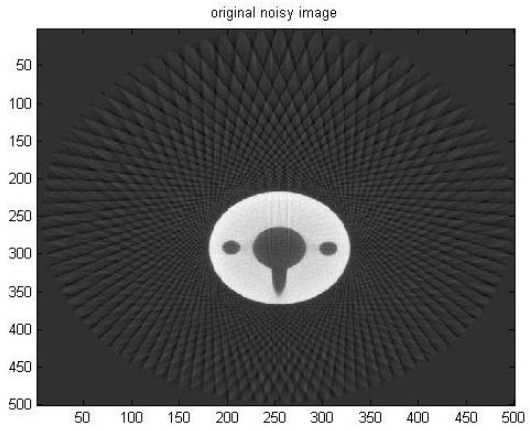

Figure 1. Streaking artifacts observed in an Industrial CT Scan image.

2. RELATED WORK

Although image de-noising has been a field of extensive study for the past many decades but no one technique has been proven to be the best for all types of noise. Different techniques have been shown to provide better results in different applications. Chang et al. [Chang2000] use adaptive wavelet thresholding to de-noise images and compare Bayes shrink with Sure shrink while Kivanc et al. [Kivanc1999] employ adaptive statistical modeling of the wavelet coefficients to perform image de-noising. Other wavelets-based methods reported in literature include the work of Portilla et al. [Portilla2003], Sendur and Selesnick [SendurSelesnick2002] and Rajpoot et al. [Rajpoot2004]. Some other transforms that have found application in de-noising is the curvelet transform [Starck2002] and the fast Fourier transform [Jain1989]. On the other hand some experts have chosen to work with multiwavelets [Bui1998]. Some spatial methods have also found application in de-noising namely non-local algorithms by Buades et al. [Baudes2005] , MDL by Rissanen [Rissanen2000] , median filtering by Yang et al. [Yang1995] and Hamza et al. [Hamza1999] , Wiener filtering by Jain [Jain1989] and bilateral mesh de-noising by Fleishman et al. [Fleishman2003] . Other methods used for de-noising include learning [Elad2006] and fractal dimensions [Ghazel2003]. In a review, Buades et al. contend that the performance of most de-noising methods is highly dependent upon the assumptions taken and the corresponding data-set used [Baudes022005]. Slight variation in the data-set results in lowering of de-noising accuracy. Motwani et al. [Motwani2004] present a survey of various techniques from the spatial as well as the transform domain and conclude that wavelets work best. However, Motwani contend that the noise in images is often assumed to be gaussian which is often not the case in the real world. One good example of such noise is the streaking noise in industrial 3DXCTs. Some work on 3DXCT scan de-noising has already been done which includes Mayer et al.'s [Mayer2007] work that compares non-linear diffusion with wavelets-based methods in de-noising medical XCT. Li et al. have found anisotropic diffusion to work well in reducing noise in industrial 3DXCTs [Li2009].

In this paper, we compare the performance of Otsu method, Fourier transforms, wavelet shrinkage and anisotropic diffusion in removing streaking artifacts from industrial 3DXCT scans. We employ a variety of data-sets and provide de-noising results using various picture quality metrics. Such a comparison for industrial 3DXCT has not been carried out in the literature before. In this paper we compare various de-noising techniques for industrial 3DXCT and present which technique works best. We also present how Otsu method may be used for de-noising. Another important contribution of the paper is the evaluation of the results using multiple quality metrics. Mean squared error used frequently for picture quality estimation has proven to be not very accurate [WangBovik2009] especially in situations where a stable ground truth is not available. Therefore, we choose to compare the results using multiple quality metrics.

3. METHODS AND TECHNIQUES

In this work, we address two important aspects related to image de-noising: The first aspect is comparison of various de-noising techniques and the

second aspect is an assessment of the picture quality metrics to evaluate the results. We discuss each aspect in the sections below:

De-noising Methods

We have used various techniques to carry out de-noising. In the subsequent sections, we discuss each technique independently:

3.1.1 Otsu Thresholding

Since the use of Otsu method for barcode de-noising by Shellhammer et al. [Shellhammer1999], not much work has been carried out using the Otsu method for de-noising. We propose to use the Otsu thresholding in a scheme similar to the one proposed by Shellhammer et al. to de-noise a 3DXCT scan image. Since there is a great variation in the Hounsfield units obtained in industrial 3DXCT, adaptive automatic thresholding as proposed by Otsu [Otsu1975] can provide interesting insights as to how to de-noise images. We use the method to acquire a de-noised version of the industrial 3DXCT scan.

3.1.2 Fourier Transform

Fourier transform converts a signal from the time domain in to the frequency domain referred to as the Fourier space. In this paper, we use the Fourier space just as in the curvelet transform to acquire the frequency pattern for streaking artifacts and then remove the artifacts by removing frequencies associated with the noise. Application of 2D Fourier transform for image de-noising is carried out by removing the high frequency components as described by Gonzalez and Woods [Gonzalez2002]. Low pass filtering is applied using a 7 pixel circular filter.

3.1.3 Wavelet Shrinkage

We use the standard wavelet shrinkage method as proposed by Donoho and Johnstone [Donoho1995]. The selection of threshold is carried out using the Birge and Massart method [BirgeMassart1997]. We use various shrinkage functions namely soft, hard and garrote as suggested by Fodor and Kamath [FodorKamath2003]. The results for each are presented.

Daubechies 4-tap filter is used for wavelets analysis. Other wavelets were also tried but Daubechies combined with Birge and Massart method produces the best results. Other threshold calculation methods such as Sure, Bayes and Penalized were also attempted but no improvements in results were seen.

3.1.4 Anisotropic Diffusion

Anisotropic diffusion also referred to as Perona-Malik diffusion [Perona1990] is a powerful technique for removing noise from an image while preserving important information such as edges and other details. It has been known to perform well for medical imaging. The filtering is carried out for 100 iterations.

Picture Quality Metrics

We use various quality metrics for acquiring an estimate of the quality of the picture obtained after de-noising. The ground truth is obtained from scanning the object in question at high resolutions. However the ground truth is not entirely noise free. The performance of the various techniques is measured using six metrics, namely Peak Signal to Noise Ratio (PSNR), Structural Similarity Index Metric (SSIM), Chou and Li Metric (CLM) [Mayache1998], Czenakowski Distance (CZD) and Spectral Magnitude Distortion (SMD) [DosselmannYang2005]. The reason for using multiple metrics is that each represents the de-noising performance of the technique used, in terms of different properties of the acquired image. PSNR and SSIM consider the global differences between the image and the ground truth, while CLM represents the visual quality of the image with the help of JND (Just Noticeable Distortion). On the other hand, CZD and SMD consider global correlation and global spectral analysis respectively.

4. RESULTS AND DISCUSSION

We tested three data-sets to analyze the effect of the various de-noising algorithms. Some images from each data-set are shown in the Figure 2. These image-sets will be referred to as *Kalibrierkorper_LR_0* (simple geometrically shaped mono-material), *KF9_real* (complex geometrically shaped mono-material) and *Testkörper_TK08* (simple geometrically shaped bi-material, metal and plastic).

Completely noiseless data is not available to us, as even with very high number of projections industrial CT-scanned images still contain some noise. In our analysis we took the least noisy image as the ground-truth and evaluated the performance of de-noising methods by comparing the ground truth image with the de-noised one.

Ground truth is obtained using increased number of projections. As stated earlier, one of the major source of streaking artifacts is the insufficient number of projections taken during a CT scan. Industrial 3DXCT machines take multiple x-ray images (projections) of a specimen in a single 360 degree rotation of the machine about the specimen. These projections are then used to compute a 3D volumetric data set for the specimen. The number of projections taken in one 360 degrees rotation about the specimen directly affect the amount of streaking artifacts present in the data set. Less number of projections result in more streaking artifacts due to insufficient sampling rate whereas streaking artifacts reduce as the number of samples (projections) are increased.

The ground truth in our analysis is obtained using a very high number of projections.

In Table 1, 2 and 3, the results of different de-noising techniques on data sets *Kalibrierkorper_LR_0*, *KF9_real* and *Testkörper_TK08* using various quality metrics are shown respectively.

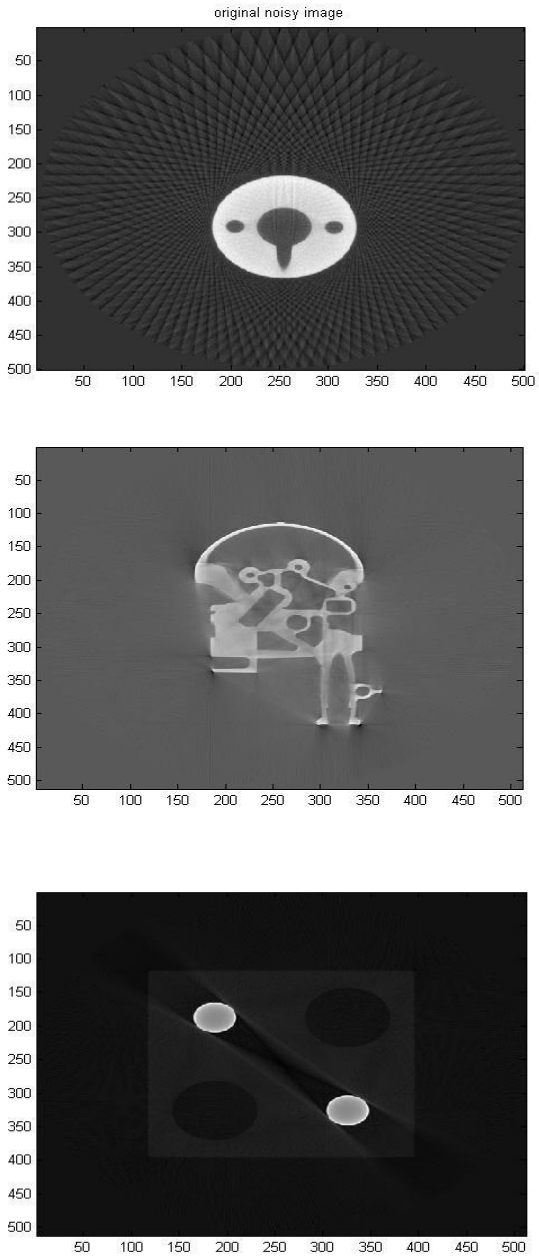

Figure 2. 50th Slice of Kalibrierkorper_LR_0, 300th slice of *KF9_real*, 150th slice of *Testkörper_TK08*

The various quality metrics represent different aspects pertaining the de-noised results. PSNR is a very good metric for estimating the quality of images reconstructed from lossy image CODECs and estimating the quality of transmitted data. It may not be the best metric in this instance due to the nature of the problem as described earlier and also due to the fact that PSNR is closely related to MSE which is not the best metric in problems such as ours. For image and video compression PSNR in the range of 30dB to 50 dB is generally considered good. The PSNR values for the de-noised image in Table 1 and Table 3 indicates that the technique has improved the quality of the image. However, the results for second data-set i.e. *KF9_real* are not very good as they lie between 7 dB to 25.4 dB. As per PSNR Otsu method is consistently the worst method. PSNR values indicate that although some de-noising has been obtained for *KF9_real* but it is not too much improvement. This is also evident from de-noised images in Figures 1-8.

	O	**F**	**Ws**	**Wh**	**Wg**	**A**
PSNR	6.5	27.8	43.9	43.3	43.7	**48.2**
SSIM	0.13	0.96	**0.99**	0.98	0.98	**0.99**
CLM	3555	25.13	0.23	0.30	0.23	**0.07**
CZD	0.875	0.018	0.003	0.004	0.003	**0.002**
SMD	$2.5X\ 10^{14}$	$1.9X\ 10^{12}$	$5.9X\ 10^{10}$	$5.3X\ 10^{10}$	$\mathbf{5.2X\ 10^{10}}$	$1.7X\ 10^{16}$

Table 1. Metric results for *Kalibrierkorper_LR_0* are shown where 'O' stands for Otsu threshold, 'F' for fourier filtering, 'Ws' for soft wavelet thresholding, 'Wh' for hard wavelet thresholding, 'Wg' for garrotte thresholding and 'A' for anisotropic diffusion

	O	**F**	**Ws**	**Wh**	**Wg**	**A**
PSNR	7.79	23.3	**25.4**	**25.4**	**25.4**	**25.4**
SSIM	0.03	0.94	**0.98**	**0.98**	**0.98**	**0.98**
CLM	2663	69	**41**	**41**	**41**	**41**
CZD	0.97	0.08	**0.07**	**0.07**	**0.07**	**0.07**
SMD	$1.9X\ 10^{14}$	$5.3X\ 10^{12}$	$\mathbf{3.3X\ 10^{12}}$	$\mathbf{3.3X\ 10^{12}}$	$\mathbf{3.3X\ 10^{12}}$	$\mathbf{3.3X\ 10^{12}}$

Table 2. Metric results for *KF9_real* are shown where 'O' stands for Otsu threshold, 'F' for fourier filtering, 'Ws' for soft wavelet thresholding, 'Wh' for hard wavelet thresholding, 'Wg' for garrotte thresholding and 'A' for anisotropic diffusion

	O	**F**	**Ws**	**Wh**	**Wg**	**A**
PSNR	0.21	**33.2**	32.2	32.2	32.2	32.0
SSIM	0.21	**0.98**	**0.98**	**0.98**	**0.98**	0.97
CLM	359	**4.6**	9.1	9.1	9.1	9.5

CZD	0.81	**0.03**	0.06	0.06	0.06	0.06
SMD	2.6X 10^{13}	**5.9X 10^{11}**	7.4X 10^{11}	7.4X 10^{11}	7.4X 10^{11}	7.7X 10^{11}

Table 3. Metric results for *Testkörper_TK08* are shown where 'O' stands for Otsu threshold, 'F' for Frequency Filtration, 'Ws' for Soft wavelet Thresholding, 'Wh' for hard Wavelet Thresholding, 'Wg' for Garrotte Thresholding, and 'A' for anisotropic diffusion

SSIM or the Structural Similarity Index Metric as the name suggests measures the structural similarity between the noisy and de-noised image. It is considered an improvement over PSNR and MSE as it does not compare the whole image but looks for structural similarity. A value of 1 for SSIM indicates a complete match i.e. the images being compared are identical. Results in Table 1, 2 and 3 indicate that soft thresholding based wavelet shrinkage performs very well for all data-sets producing a SSIM of 0.99, 0.98 and 0.98 followed by anisotropic diffusion. Different thresholding techniques for wavelet shrinkage also produce high SSIM values. Fourier transform has also produced good results but not as good as wavelet shrinkage and anisotropic diffusion. The results indicate that wavelet shrinkage, anisotropic diffusion and Fourier transform maintain the image structure in the de-noising process. However, Otsu is the worst technique as the results indicate that Otsu method has significantly modified the image structure in the de-noised image.

CLM provides an estimate of image quality in terms of distortion accrued in the de-noised image in the process of de-noising in comparison with the ground truth. Lower the distortion the better the results. The values for CLM vary greatly for different data-sets as can be seen in Table 1, 2 and 3. The CLM metric indicates that de-noising works best for the first data-set i.e. *Kalibrierkorper_LR_0*. This fact is interestingly also evident from the results in Figures 1-8. The best value for CLM in the case of *Kalibrierkorper_LR_0* is obtained for anisotropic diffusion which is 0.07 which contrast greatly from 41 and 4.6 for other data-sets. An important aspect to note is that CLM metric also indicates that Fourier transform works best for the last data-set i.e. *Testkörper_TK08*. Very high values for CLM are obtained in the case of Otsu method indicating that the technique does not work well at all for 3DXCT scanned images de-noising.

CZD or Czenakowski Distance measures the percentage of similarity between two images which in this case are the de-noised image and the ground truth. As the difference between two images tends to zero the more similar the images are. The results in Tables 1, 2 and 3 indicate that except for Otsu method all other techniques produce very low values for CZD with anisotropic diffusion producing the best results for *Kalibrierkorper_LR_0***.** However, the difference between de-noising results for *Kalibrierkorper_LR_0* and other data-sets is quite large in terms of CZD as it is more than 10 times as compared to *Kalibrierkorper_LR_0* (with the exception of Otsu method which again produces very poor results). This result also indicates that de-noising works best for data-sets such as *Kalibrierkorper_LR_0* which can also be seen from the images in Figures 1-8.

SMD measures the quality of the de-noised image in the spectral i.e. frequency domain. The lower the difference the better the results. It can be seen that very high values for SMD are obtained for all data sets indicating that there is still a presence of considerable noise. The values for SMD confirm for the two data-sets namely *KF9_real* and *Testkörper_TK08* that wavelet shrinkage and anisotropic diffusion produce similar results and Fourier transform is the best technique for the latter. However, the SMD results for *Kalibrierkorper_LR_0* are most interesting in the sense that it indicates that garrote thresholding based wavelet shrinkage produces the best results which is a deviation from what other metrics indicate. This may be due to the fact that SMD is unable to detect localized errors as the Fourier transform estimates the total energy of the signal.

From the above discussion it can be concluded that best de-noising results may be obtained for data-sets such as *Kalibrierkorper_LR_0*. However, for other data-sets the improvement in quality is only marginal but some techniques tend to keep the structural integrity intact while others such as Otsu compromise it.

The results in Tables 1, 2 and 3, clearly indicate that the Otsu's metric results are not very good for all types of 3DXCT scan images. Figure 3 shows the performance of the Otsu method on 50th slice of *Kalibrierkorper_LR_0*, 300th slice of *KF9_real* and 150th slice of *Testkörper_TK08*. In the *Testkörper_TK08* filtered result, one can clearly see that Otsu removed the non-metal intensity value along with the air considering it to be noise.

Moreover, for mono materials (in Table 1 & 2) the metrics index for Fourier filtering are much better when compared with Otsu. However, blurring is observed as some important edges are removed but in bi-materials case i.e. *Testkörper_TK08* (Table 3), Fourier filtering was found to be the best method based upon most of the metrics (except SSIM). In the case of bi-material based structure, the object is so badly corrupted by streaking noise that according to our metrics, no other de-noising technique improved the quality of the image.

We applied wavelet filtering using Daubechies 2 wavelet up to level 9 while threshold was calculated using Birge and Massart method. It improved our results for the geometrical shaped mono material *(Kalibrierkorper_LR_0*) to a certain level but improvement for complex geometrically shaped mono-materials (*KF9_real*) was very low and it proved almost useless for simple geometrically shaped bi-material (*Testkörper_TK08*). Among wavelets we found soft thresholding results to be the best for the first data set. For the other two data-sets, the different wavelet thresholding methods produced identical results. Anisotropic diffusion provides the best results for the first two image data sets. Therefore, anisotropic diffusion is the best method for de-noising of mono material 3DXCT scanned images. But it did not work well for *Testkörper_TK08*.

The reason why anisotropic diffusion and wavelet shrinkage work better than other techniques for removing streaking artifacts is probably because both techniques are multi-resolution in nature and allow for removal of noise artifacts at different scale-space resolutions. This is particularly important in the case of streaking artifacts as they represent noise at multiple frequencies which is captured well using various scale-space resolutions. Hence, once the noise is de-correlated at various scale-space resolutions, the de-noising is more accurate as the noise is removed separately at each scale space. At the same time, another additional feature of anisotropic diffusion is that it adapts to the local noise variations by suppressing the noise and enhancing the texture. Therefore, anisotropic diffusion is able to surpass wavelet shrinkage in removing streaking artifacts.

Moreover, we have also compared the methods in terms of the time they took to perform the de-noising. Table 4 shows the processing time for each technique. Otsu is the fastest but as discussed before does produce very good results. Wavelet shrinkage offers the best compromise with acceptable results and very quick processing time of 40 seconds. Fourier filtering takes 5 minutes but Anisotropic Diffusion takes the most amount time of more than an hour although it produces the best results in terms of quality. Speed of a technique is important as a typical 3DXCT scan contains hundreds and thousands of images.

	Processing Time
Anisotropic Diffusion	1 hour 2 sec
Fourier Filtering	5 min
Wavelets	40 sec
Otsu	28.6 sec

Table 4. Processing time for various techniques for de-noising 256 slices of a 512X512 XCT Scan

5. CONCLUSIONS

This paper compares established techniques in de-noising literature for removing noise in industrial 3DXCT scan data. 3 different data-sets are used and the efficacy of the technique on these 3 data-sets is investigated and compared using different picture quality metrics.

The analysis shows that anisotropic diffusion produces the best results while wavelet shrinkage provides the second best results. Often the wavelet shrinkage results are as good as anisotropic diffusion. Frequency space based techniques such as the Fourier transform works well in situations where the original image has been greatly compromised by streaking artifacts otherwise anisotropic diffusion and wavelet shrinkage are better techniques. Otsu thresholding has been found to be not a very good technique for industrial 3DXCT de-noising. However, it is important to note that the improvement in quality is only marginal for most data-sets included in the study. Great improvement in quality can be seen for the first data-set. In terms of speed and accuracy, wavelet shrinkage provides the best compromise.

Our future work would include comparing other de-noising techniques with anisotropic diffusion and wavelet shrinkage based methods and also to come up with new techniques that can produce good and robust de-noising results.

6. ACKNOWLEDGMENTS

Our thanks to Higher Education Commission Pakistan for funding this research work.

7. REFERENCES

[Chang2000] Chang, S.G., Yu, B. and Vetterli, M. Adaptive wavelet thresholding for image de-noising and compression. IEEE Transactions on Image Processing, , pp. 1532–1546, (2000).

[Kivanc1999] Kivanc, M., Kozintsev, I. Ramchandran, K. and Moulin, P. Low-complexity image de-noising based on statistical modeling of wavelet coefficients. IEEE Signal Processing Letters, Vol. 6, pp. 300–303, (1999).

[Portilla2003] Portilla, J., Strela, V., Wainwright, M.J. and Simoncelli, E.P. Image de-noising using scale mixtures of Gaussians in the wavelet domain. IEEE Transactions on Image Processing, Vol. 12 pp. 1338-1351, 2003.

[SendurSelesnick2002] Sendur, L. and Selesnick, I.W., Bivariate shrinkage functions for wavelet-

based de-noising exploiting inter-scale dependency. IEEE Transactions on Signal Processing, vol. 50, no. 11, pp.2744-2756, 2002.

[Rajpoot2004] Rajpoot, N., Yao, Z. and Wilson, R., Adaptive wavelet restoration of noisy video sequences. International Conference on Image Processing, 2004. ICIP'04. 2004 vol. 2, pp.957-960, 2004.

[Starck2002] Starck, J.L., Candes, E.J., Donoho, D.L. The curvelet transform for image de-noising. IEEE Transactions on Image Processing, vol. 11, pp.670-684, 2002.

[Jain1989] Jain, A.K. Fundamentals of digital image processing. Prentice-Hall, Inc. 1989.

[Bui1998] Bui, T.D. and Chen, G. Translation-invariant de-noising using multiwavelets. IEEE Transactions on Signal Processing, vol. 46, pp.3414-3420, 1998.

[Baudes2005] Buades, A., Coll, B. and Morel, J.M. A non-local algorithm for image de-noising. IEEE Computer Society Conference on Computer Vision and Pattern Recognition, 2005. CVPR 2005. vol. 2, pp.60-65, 2005.

[Rissanen2000] Rissanen, J. MDL de-noising. IEEE Transactions on Information Theory, vol. 46, pp. 2537-2543, 2000.

[Yang1995] Yang, R., Yin, L., Gabbouj, M., Astola, J. and Neuvo, Y. Optimal weighted median filtering under structural constraints. IEEE Transactions on Signal Processing, vol. 43, no. 3, pp.591-604, 1995.

[Hamza1999] Hamza, A.B., Luque-Escamilla, P.L., Martinez-Aroza, J. and Roman-Roldan,R. Removing noise and preserving details with relaxed median filters. Journal of Mathematical Imaging and Vision, vol.11, pp.161-177, 1999, Springer.

[Fleishman2003] Fleishman, S., Drori, I. and Cohen-Or, D. Bilateral mesh de-noising. ACM Transactions on Graphics, vol.22, pp.950-953, 2003.

[Elad2006] Elad, M. and Aharon, M. Image de-noising via sparse and redundant representations over learned dictionaries. IEEE Transactions on Image Processing, vol.15, pp.3736-3745, 2006.

[Ghazel2003] Ghazel, M., Freeman, G.H. and Vrscay, E.R. Fractal image de-noising. IEEE Transactions on Image Processing, vol. 12, pp.1560-1578, 2003.

[Baudes022005] Buades, A., Coll, B. and Morel, J.M. A review of image de-noising algorithms, with a new one. SIAM Journal on Multiscale Modeling and Simulation, vol. 4, pp.490-530, 2005.

[Motwani2004] Motwani, M.C., Gadiya, M.C., Motwani, R.C. and Harris Jr, F.C. Survey of image de-noising techniques. GSPx, pp.27-30, 2004.

[Mayer2007] Mayer, M., Borsdorf, A., Köstler, H., Hornegger, J. and Rüde, U. Nonlinear Diffusion vs. Wavelet Based Noise Reduction in CT Using Correlation Analysis. Vision, Modeling, and Visualization, pp.223-232, 2007.

[Li2009] Li, J., Wang, L. and Bao, P. An industrial CT image adaptive filtering method based on anisotropic diffusion. International Conference on Mechatronics and Automation, 2009. pp.1009-1014, 2009.

[WangBovik2009] Wang, Z. and Bovik, A.C. Mean squared error: Love it or leave it? A new look at signal fidelity measures. Signal Processing Magazine, IEEE, pp.98-117, 2009.

[Shellhammer1999] Shellhammer, S.J. and Goren, D.P. and Pavlidis, T. Novel signal-processing techniques in barcode scanning. IEEE Robotics & Automation Magazine, vol. 6, pp.57-65, 1999.

[Otsu1975] Otsu, N. A threshold selection method from gray-level histograms. Automatica, vol. 11, pp.285-296, 1975.

[Gonzalez2002] Gonzalez, R.C. and Woods, R.E. Digital image processing. Prentice Hall, 2002.

[Donoho1995] Donoho, D.L., Johnstone, I.M., Kerkyacharian, G. and Picard, D. Wavelet shrinkage: asymptopia? Journal of the Royal Statistical Society, Series B (Methodological), pp.301-369, 1995.

[BirgeMassart1997] Birgé, L., Massart P. From model selection to adaptive estimation. D. Pollard (ed), Festchrift for L. Le Cam, Springer, pp. 55–88, (1997).

[FodorKamath2003] Fodor, I.K. and Kamath, C. De-noising through wavelet shrinkage: an empirical study. Journal of Electronic Imaging, volume 12, pp.151, 2003.

[Perona1990] Perona, P. and Malik, J. Scale-space and edge detection using anisotropic diffusion. IEEE Transactions on Pattern Analysis and Machine Intelligence, vol. 12, pp.629-639, 1990.

[Mayache1998] Mayache, A., Eude, T. and Cherifi, H. A comparison of image quality models and metrics based on human visual sensitivity. International Conference on Image Processing, pp.409-413, 1998.

[DosselmannYang2005] Dosselmann, R. and Yang, X.D. Existing and emerging image quality metrics. Canadian Conference on Electrical and Computer Engineering, pp.1906-1913, 2005.

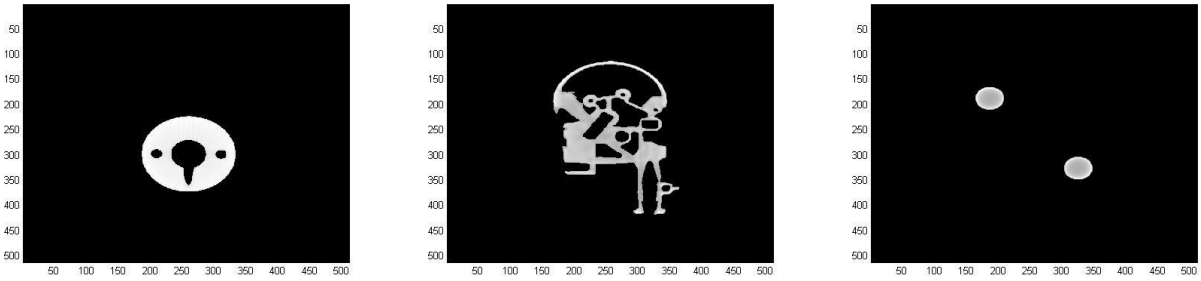

Figure 3. Denoising results for Otsu Method.

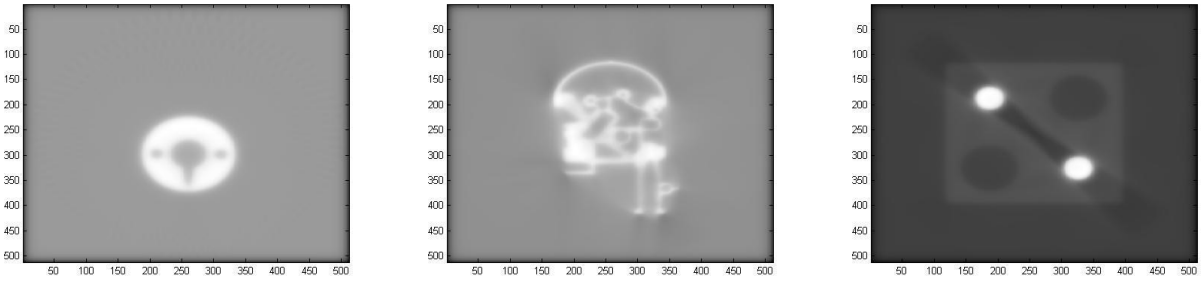

Figure 4. Denoising results for Fourier filtering.

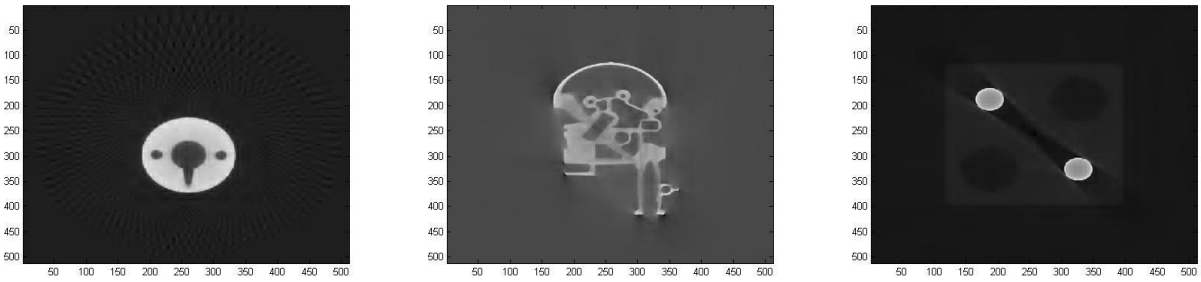

Figure 5. Denoising results for Wavelets Soft Thresholding (Daubechies filter+Birge-Massart threshold calculation).

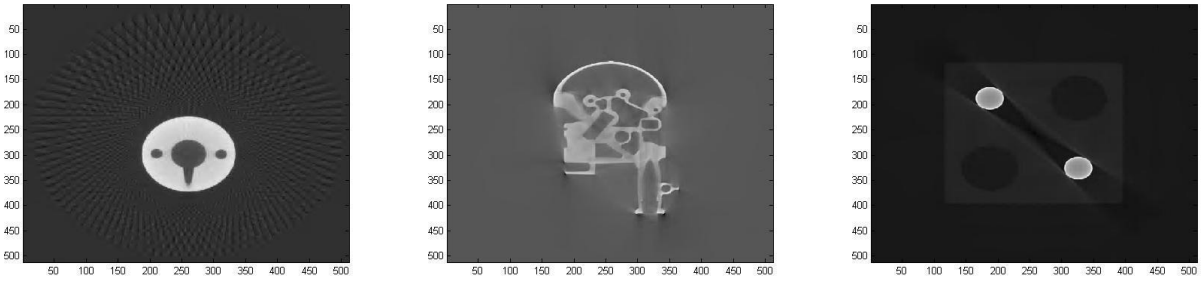

Figure 6. Denoising results for Wavelets Hard Thresholding (Daubechies filter+Birge-Massart threshold calculation).

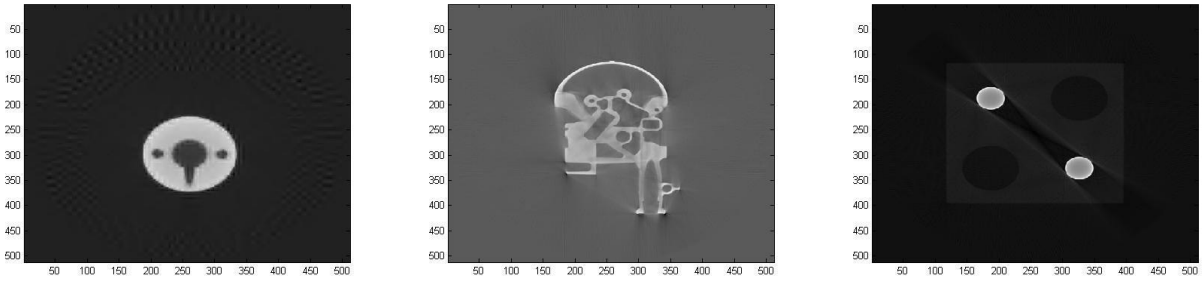

Figure 7. Denoising results for Wavelets Garrotte Thresholding (Daubechies filter+Birge-Massart threshold calculation).

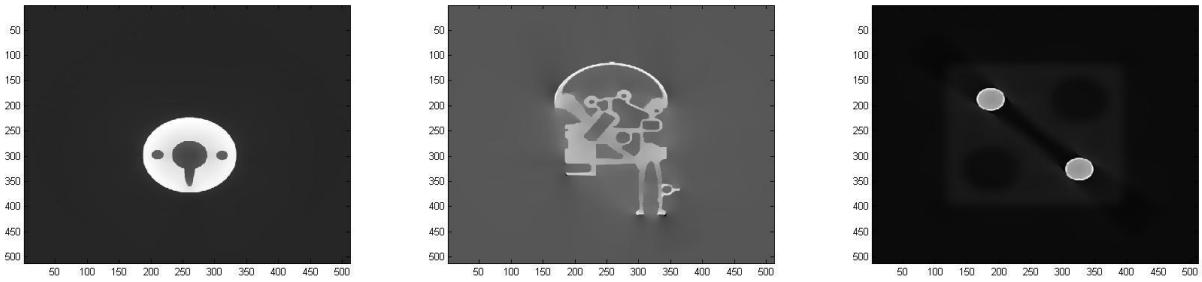

Figure 8. Denoising results for Anisotropic Diffusion.